Available online at www.sciencedirect.com
SCIENCE DIRECT®
Journal of Solid State Chemistry 178 (2005) 3522–3528
JOURNAL OF SOLID STATE CHEMISTRY
www.elsevier.com/locate/jssc

The synthesis of ZnS hollow nanospheres with nanoporous shell

Hua-Feng Shao, Xue-Feng Qian*, Zi-Kang Zhu

School of Chemistry and Chemical Technology, State Key Laboratory of Composite Materials, Shanghai Jiao Tong University, Shanghai, 200240, PR China

Received 18 July 2005; received in revised form 8 September 2005; accepted 9 September 2005
Available online 10 October 2005

Abstract

ZnS hollow nanospheres with nanoporous shell were successfully synthesized through the evolvement of ZnO nanospheres which were synthesized by hydrothermal method with poly (sodium-*p*-styrene sulfonate) (PSS) as surfactant at low temperature. The as-synthesized samples were characterized with X-ray diffraction (XRD), transmission electron microscopy (TEM), field emission scanning electron microscopy (FESEM), UV/vis spectrum and N_2 adsorption. The results showed that the shell of as-synthesized ZnS hollow structure was composed of many fine crystallites and had a nanoporous structure with pore diameter about 4 nm demonstrated by N_2 adsorption/desorption isotherm. The sample possessed efficiency of photocatalytic degradation on *X*-containing ($X = Cl$, Br, I) organic pollutants.

Keywords: Nanospheres; Hollow; Nanoporous shell; ZnS; Photocatalysis

1. Introduction

ZnS is a wide-band-gap semiconductor and a well-known luminescence material having prominent applications in displays, sensors, and lasers [1]. ZnS is also a very attractive candidate for applications in novel photonic crystal devices operating in the region from visible to near-IR owing to its excellent transmission property and its high index of refraction (2.27 at 1 μm) [2]. Due to the quantum confinement effect, the properties change dramatically compared with the bulk materials, and ZnS nanorods [3], nanowires [4,5], nanosheets [6], nanobelts [7], nanotubes [8], nanosaws [9] and nanoparticles [10,11] have been reported numerously.

Up to now, varied methods were used to synthesize the ZnS nanostructure. Liu et al. [12] synthesized radial ZnS nanoribbons through annealing the as-synthesized ZnS (0.5 en), [13] which was obtained in the ethylenediamine solution by microwave-assisted solvothermal methods. Zhao et al. [2] reported a novel and facile low-temperature solution method to synthesize hexagonal ZnS nanocrystals with the average diameters about 4.2 nm, which is calculated by the UV/vis spectrum [10]. Yue et al. [14] fabricated the monodisperse ZnS nanopheres with an average diameter about 100 nm by the hydrothermal method, and each nanosphere consists of many ultrafine particles with a mean diameter about 10 nm. Daniel et al. [9] synthesized wurtzite structured ZnS nanoribbons and nanosaws, which is suggested to be the self-catalyzed growth of the Zn-terminated (0001) surface while the S-terminated (000−1) surface is relatively chemically inactive, by a catalyst-free solid–vapor deposition technique.

Hollow spheres with nanometer-to-micrometer dimensions having tailored structural, optical, and surface properties represent an important class of materials that are potentially useful for a wide range of applications such as delivery vehicle systems, photonic crystals, fillers, and catalysts [15]. General methods for preparing ZnS hollow structure include the use of hard templates such as PS microspheres [16,17] and SiO_2 spheres [18] or self-organized surfactants as templates and emulsion synthesis [15,19]. Recently, Zhang et al. [20] synthesized ZnS hollow nanospheres through solvent-thermal methods without any surfactants or hard templates, and they found that the hollow-structured ZnS nanomaterials may have potential applications in high hydrogen gas storage, drug delivery and second-order template because of their large capacity and solubility. On the other hand, as one kind of most important photocatalyst, nano-ZnS has great applications

*Corresponding author. Fax: +86 21 54741297.
E-mail address: xfqian@sjtu.edu.cn (X.-F. Qian).

0022-4596/$ - see front matter © 2005 Elsevier Inc. All rights reserved.
doi:10.1016/j.jssc.2005.09.007

in environment protection through the removal of the organic pollutions and toxic water pollutions due to the rapid generation of the electron–hole pairs by photoexcitation and the highly negative reduction potentials of excited electrons [11].

It is well known that porous materials with high surface-to-volume ratios can be used as catalysts [21], sensor [22] and carrier [23]. Nanowires [24], nanospheres [11], and nanoparticles [25] with porous structure have been successfully prepared by interface solution deposition, template directed deposition and surfactant-assisted methods. Hu [11] fabricated ZnS nanoporous solid nanospheres through a heating reflux method at 150 °C with ethylene glycol (EG) as solvent, but it is difficult to separate the as-synthesized ZnS nanoparticles from the solvent because of the relative high viscosity of EG. In this article we report a simple solution route to synthesize ZnS hollow nanospheres with a nanoporous shell at low temperature in aqueous solution due to the Kirkendall effect [26].

2. Experimental sections

2.1. Experimental

Zinc nitrate hexahydrate ($Zn(NO_3)_2 \cdot 6H_2O$), thiourea (TU), ammonium chloride and ammonia (25%) were used as reactants without further purification. The poly (sodium-*p*-styrene sulfonate) (PSS) was purchased from ACROS organics. In a typical process, 10 mmol $Zn(NO_3)_2 \cdot 6H_2O$, 10 mmol TU, 0.03 mmol PSS and 2 mmol ammonium chloride were dissolved in 95 mL distilled water to form homogeneous solution with magnetic stirring. Then 5 mL ammonia was transferred into the above solution, the reaction solution became milky ($Zn(OH)_2$) first and then turned to clear quickly because of the formation of zinc amino complex. The above solution was transferred into a Teflon-lined stainless-steel autoclave up to 80% of volume. The sealed autoclave was maintained at 120 °C for a given time, and then cooled to room temperature naturally. The resulting product was collected by ultra-high speed centrifuge and washed several times with absolute ethanol and distilled water, then vacuum dried at 60 °C for 6 h.

2.2. Characterization

The powder X-ray diffraction (XRD) patterns were recorded at a scanning rate of $4^\circ\,min^{-1}$ in the 2θ range of 20–70° using a Shimadzu XRD-6000 X-ray diffractometer with Cu-$K\alpha$ radiation ($\lambda = 1.5406$ Å). The morphologies of the as-synthesized product were further observed using a JEOL JEM-100CXII transmission electron microscopy (TEM) at the acceleration voltage 100 kV. Energy dispersive X-ray spectrum (OXFORD INCA energy spectrometer), linked with Sirion 200 field emission scanning electron microscopy, was used to analyze the element distributions. The samples were prepared by mounting a drop of the resulting aqueous solution on carbon-coated Cu grids and allowed to dry in air. Selected area electron diffraction (SAED) was also recorded on the JEOL TEM. Adsorption isotherms were obtained using a micromeritics ASAP 2010 porosimeter. The specific surface area, A_{BET}, was determined from the linear part of the BET equation. The calculation of the porous size distribution was performed using the desorption branches of the N_2 desorption isotherms. Photocatalytic activity measurement was performed as follows: 0.01 mmol eosinB (Shanghai Chemical Reagent Corp.) and 0.1 mmol the obtained ZnS hollow sphere were dispersed in distilled water by magnetic stirring to reach the adsorption equilibrium of eosinB and ZnS, and then exposed under high-pressure Hg lamp (250 W) with different reaction times before UV/vis testing. UV/vis absorption spectra were collected using Perkin-Elmer Lambda 20 UV/vis spectrophotometer.

3. Results and discussion

Fig. 1 presents typical TEM and FESEM images of hollow ZnS nanospheres with nanoporous shell that were obtained at a PSS concentration of 0.3 mmol L^{-1}. The low-magnification TEM image, Fig. 1a, shows that the hollow spheres are rather uniform with an average diameter about 120 nm and a shell thickness about 20–30 nm. Some unperfect hollow spheres also can be seen in the images because the shell of the nanospheres is relatively weak and easy to crack under the collision due to the vigorous convection of the solution under high temperature and pressure. From the TEM image, it also can be seen that the cracked nanospheres also tended to form the "8" configuration during further growth of the crystallites. From the magnified TEM image (Fig. 1b), it can be clearly found that the shell of the single nanospheres was rough and composed of a large quantity of small well-dispersed spherical nanocrystals with uniform size and shape (see Fig. 1b labeled with circles). The average diameter of these nanocrystals is about 8 nm and they assembled in a nanoporous structure. The FESEM analysis also can demonstrate this. Fig. 1c shows the FESEM of the as-synthesized sample. It can be seen that the surface of the nanospheres is rough and uneven. Some little particles with diameters about 8 nm can be seen on the surface. According to the Scherrer equation, the average size of the ZnS crystalline is about 7.5 nm, which is close to the value observed by electron microscopy. The SAED pattern (inset of Fig. 1b) shows a serial of discontinuous concentric rings that were composed of some spots because of the much more small particles. The diffraction rings can be indexed to (111), (220) and (311) planes of the cubic ZnS phase (JCPDS No. 80-20).

In the experimental process, the reaction time also has influence on the phase of the as-obtained sample. Fig. 2 shows the XRD patterns of the obtained sample at different experiment times. When the reaction time is short to 30 min, the XRD diffraction peaks of the obtained

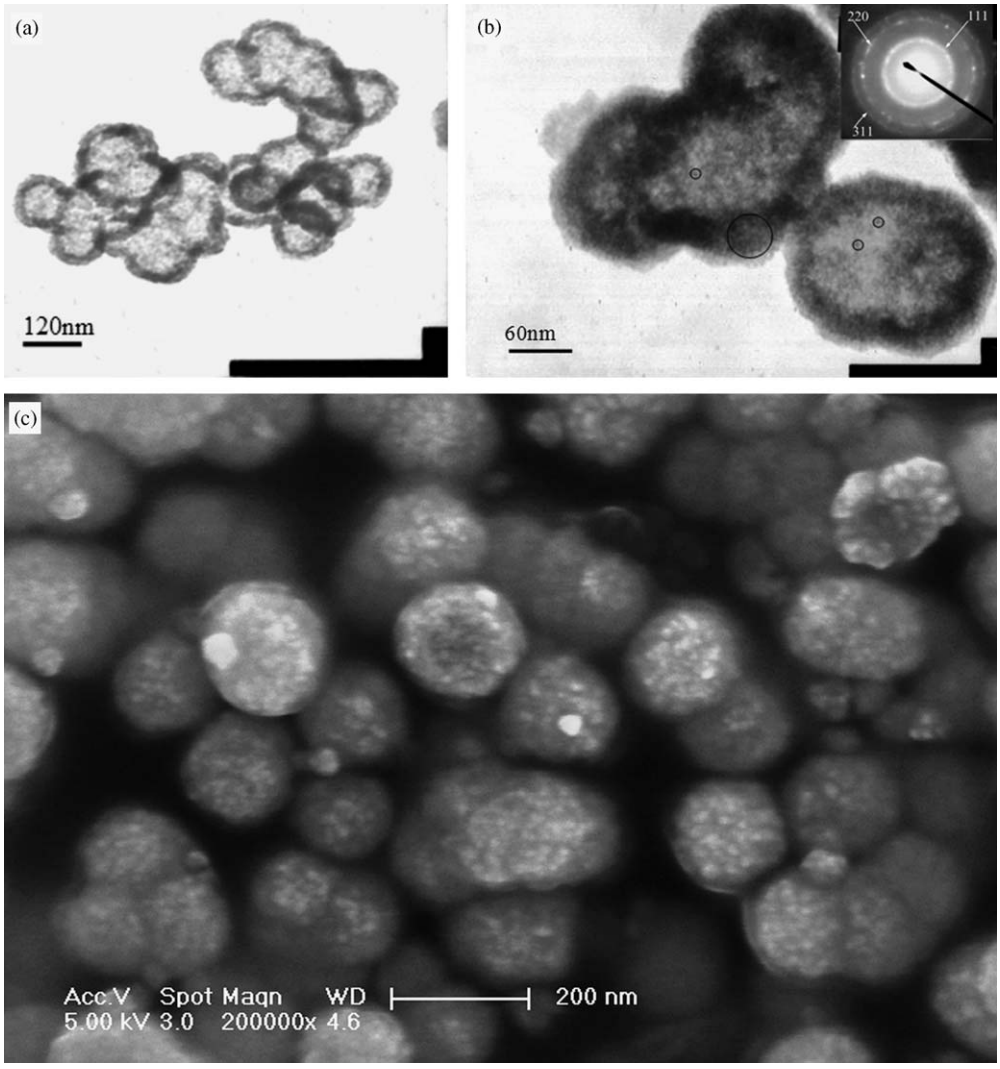

Fig. 1. TEM and FESEM images of as-obtained ZnS hollow nanopheres. (a) Low-magnification, (b) high-magnification (c) FESEM image. The inset in (b) is the selected area electron diffraction pattern. *The circles show the small ZnS particles which formed the shell.

product can be indexed to hexagonal ZnO (space group: $p63mc$ (No.186)) with lattice constants $a = 3.25$ and $c = 5.21$ Å (JCPDS No. 36-1451). Increasing the reaction time to 2 h, the diffraction peaks of ZnS appeared and the intensity of the diffraction peaks of ZnO weakened because of the phase transition from ZnO to ZnS. When reaction time is increased to 8 h, the diffraction peaks of ZnO become very weak compared to that of ZnS. Further prolonging the reaction time to 18 h, the diffraction peaks of ZnO disappeared and all the diffraction peaks well correspond to the characteristic diffractions of cubic phase ZnS. This implied that all the ZnO nanoparticles changed to cubic ZnS (JCPDS No. 80-20) with lattice constant $a = 5.35$ Å. The significant broadening of the diffraction peaks can be ascribed to the very small ZnS crystallite size within the shell of the ZnS hollow spheres [2,11]. The EDX (energy dispersive X-ray spectrum) analysis shows that the hollow spheres are composed of Zn and S element and the element ratio of Zn:S equals to 1:1 (see Supporting materials S1).

Fig. 3 shows the TEM images of the as-obtained products with the change of the reaction time. The morphology evolvement of the products provided detailed information on the crystallization process. When the reaction time was shorter than 30 min, the as-synthesized ZnO crystals (analyzed by XRD pattern above) were in lamellar substance without regular morphology (see supporting material S2). Prolonging the reaction time to 2 h, spherical nanoparticles with an average size of 120 nm were obtained (Fig. 3a). Further increasing the reaction time to 18 h, hollow structure (Fig. 3b) appeared with various thickness of the shell due to the different extent of the reaction. When the reaction time is up to 72 h, much more hollow ZnS nanospheres (Fig. 3c) appeared, in which some solid spheres still existed in the products due to the dissociative Zn^{2+} in the aqueous solution reacted with the S^{2-}. From the analysis of XRD patterns above, it can be deduced that the solid sphere is not ZnO nanosphere but the ZnS crystals. In order to demonstrate this assumption, a 5-day experiment was adopted. From the TEM images

(Fig. 3d), the hollow ZnS nanospheres changed to solid nanospheres absolutely with the uniform diameter of about 120 nm after increasing the reaction time to 5 days.

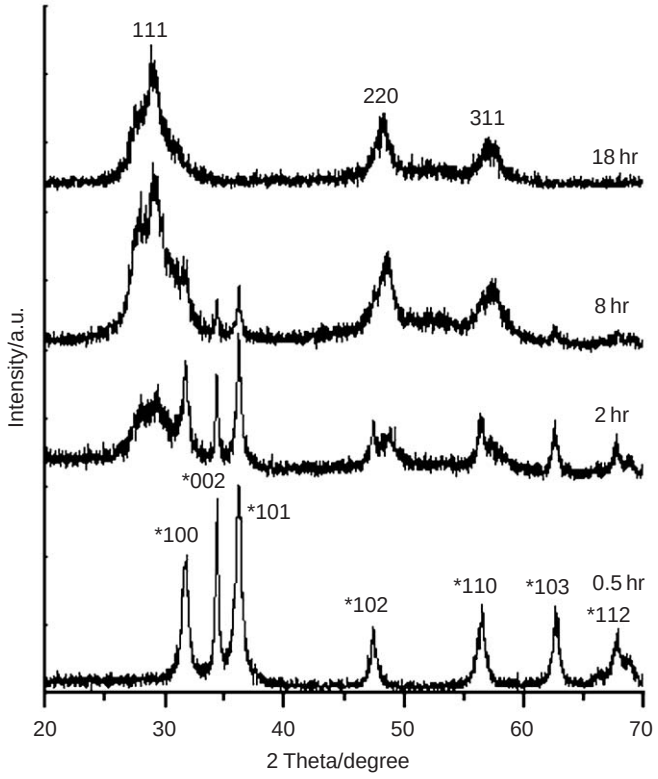

Fig. 2. X-ray diffraction patterns of the obtained products at different times. *Reaction temperature: 120 °C.

The reaction temperature also plays an important role in the phase and morphologies of the as-synthesized products. Fig. 4 is the XRD patterns of the products prepared at 100 °C. The XRD pattern of the product can be indexed to hexagonal ZnO (JCPDS No. 36-1451) exactly without any diffraction peaks of ZnS at 120 °C when reaction time is 2 h (Fig. 2) due to the slower rate of the dissolution of TU and release of S^{2-}at 100 °C. According to Chen [3], TU can dissolve in water and release S^{2-} ions in aqueous solution rapidly at elevated temperature under hydrothermal process [3], so it needs more time for the transformation of ZnO to ZnS at 100 °C compared with that at 120 °C. According to the XRD patterns and the discussion above,

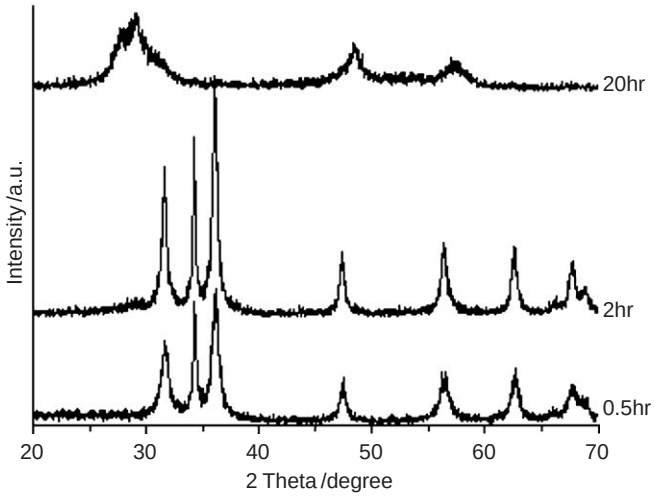

Fig. 4. X-ray diffraction patterns of the obtained products in different times. *Reaction temperature: 100 °C.

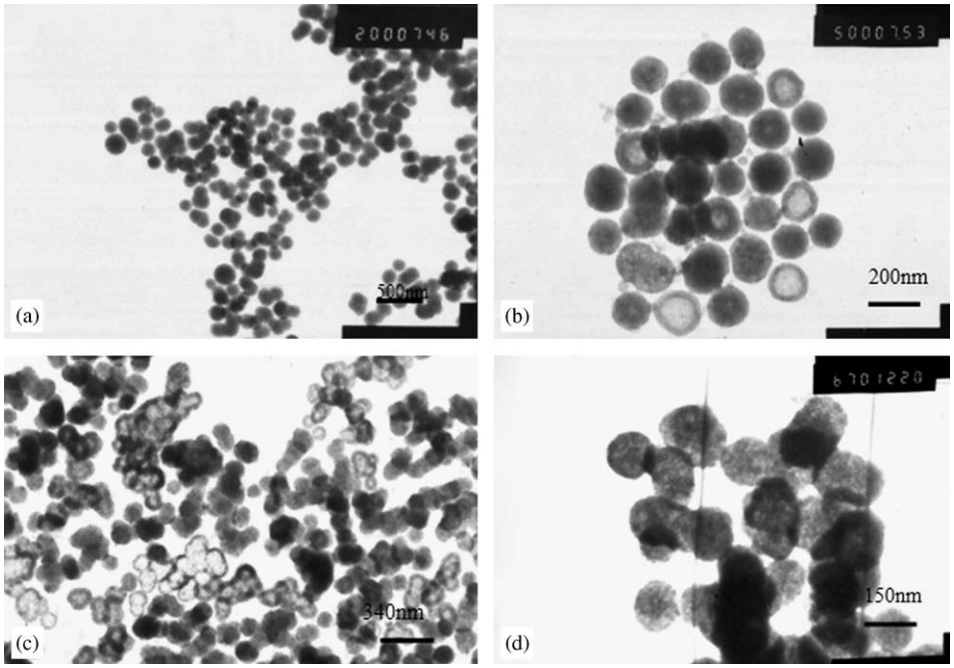

Fig. 3. TEM images of the as-synthesized products in different times. (a) 2 h; (b) 18 h; (c) 72 h; (d) 5 days

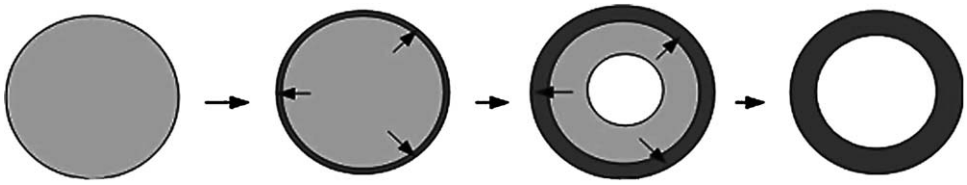

Scheme 1. Schematic illustrations of the evolvement of ZnO nanospheres to hollow ZnS nanospheres. Gray represents ZnO and dark gray represents ZnS; the arrow is the diffusion direction of Zn^{2+} and the formation process of ZnO.

we deduce the formation of the ZnS as follows: at the very short initial stage, the ZnO nanoparticles formed by the reaction between $Zn(NH_3)_4^{2+}$ and OH^-. At the same time, TU hydrolyzed and released S^{2-} under elevated temperature and pressure. Because of the thermodynamic constant of ZnO (ΔG (f_0) (400 K) $= -366\,KJ\,mol^{-1}$) is bigger than that of ZnS (ΔG (f_0) (400 K) $= -220\,KJ\,mol^{-1}$) [27], the formation of ZnO is preferential than ZnS at the same experimental condition. And then ZnO or Zn^{2+} reacted with S^{2-} to form ZnS nanocrystals. The formation of ZnS can be described as follows:

$$2OH^- + Zn(NH_3)_4{}^{2+} = ZnO(s) + H_2O + 4NH_3,$$

$$H_2NCSNH_2 + 2H_2O = CO_2 + H_2S + 2NH_3,$$

$$ZnO/Zn^{2+} + H_2S/S^{2-} = ZnS + H_2O.$$

The formation mechanism of the hollow ZnS spheres with nanoporous shell can be explained by Kirkendall process, which normally refers to comparative diffusive migrations among different atomic species in metals and/or alloys under thermally activated conditions [26], and very recently, a process analogous to the Kirkendall phenomenon has been successfully developed for nanoscale fabrication of a variety of hollow crystals [28,29]. As analyzed above, lamellar ZnO, formed at the very early stage, transferred to spherical nanoparticles with the presence of PSS, and then the obtained spherical ZnO nanoparticles were transferred to ZnS hollow structure by a direct reaction of S^{2-} with the surface layer of ZnO in the presence of water firstly. Then the Zn^{2+} inside diffuses to the solid–liquid interfaces and reacts with S^{2-} to form ZnS. In the other hand, The S^{2-} also diffuses into the inside of ZnS interface and reacts with Zn^{2+} to form ZnS. Because the size of S^{2-} is larger than that of Zn^{2+}, hollow structure is formed. The formation process was described in Scheme 1.

In the preparation process, PSS also plays an important role. With the increasing of PSS ([PSS]), the morphologies of ZnS changed from spherical conglomeration (Fig. 5a) to uneven solid and hollow spheres (Fig. 5b), and then to the uniform hollow spheres with nanoporous shell (Fig. 1). The presence of certain amount of PSS was to prevent the nanoparticles from aggregating.

In order to further study the porous structure, Brunauer–Emmett–Teller (BET) gas sorptometry measurements were conducted. Fig. 6 shows the N_2 adsorption/desorption isotherm and the pore-size distribution (inset)

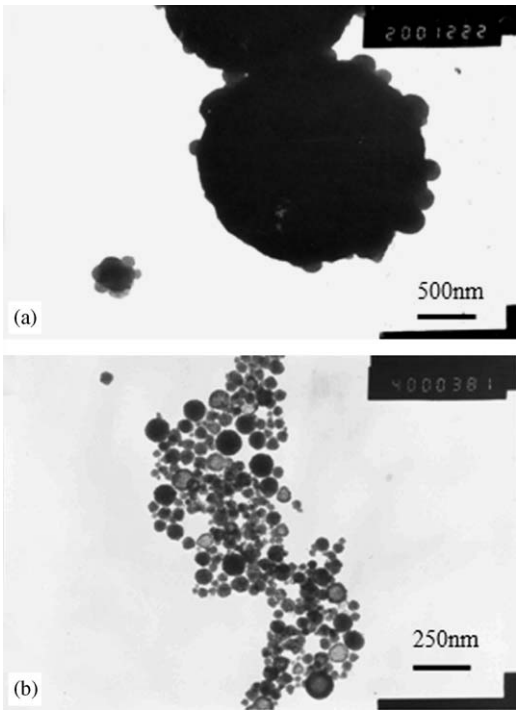

Fig. 5. TEM images of the as-synthesized ZnS with different concentrations of PSS: (a) [PSS] $= 0.02\,mmol\,L^{-1}$, (b) [PSS] $= 0.1\,mmol\,L^{-1}$.

of ZnS. The isotherms can be identified as type IV, which is characteristic of nanoporous materials. The pore-size distribution obtained from the isotherm indicates most of the pore is in 3.7 nm. These pores presumably arise from the spaces among the small nanocrystallites within the shell of a single ZnS hollow sphere. The BET specific surface area of the sample was about $97\,m^2\,g^{-1}$. Both the pore-size and the BET specific surface area show that the ZnS hollow nanospheres have a nanoporous structure.

It is well known that ZnS can be used as a semiconductor-type photocatalyst for the photoreductive dehalogenation of halogenated benzene derivatives, photocatalytic degradation of water pollutants, and photocatalytic reduction of toxic metal ions [11]. To demonstrate the potential applicability of the obtained nanoporous shell ZnS hollow nanospheres in these applications, the photocatalytic activity of the obtained ZnS nanocrystals were studied according to the literature [11]. In this process eosin B was chosen as a test agent because the bromine group can be degraded by ZnS and the characteristic absorption

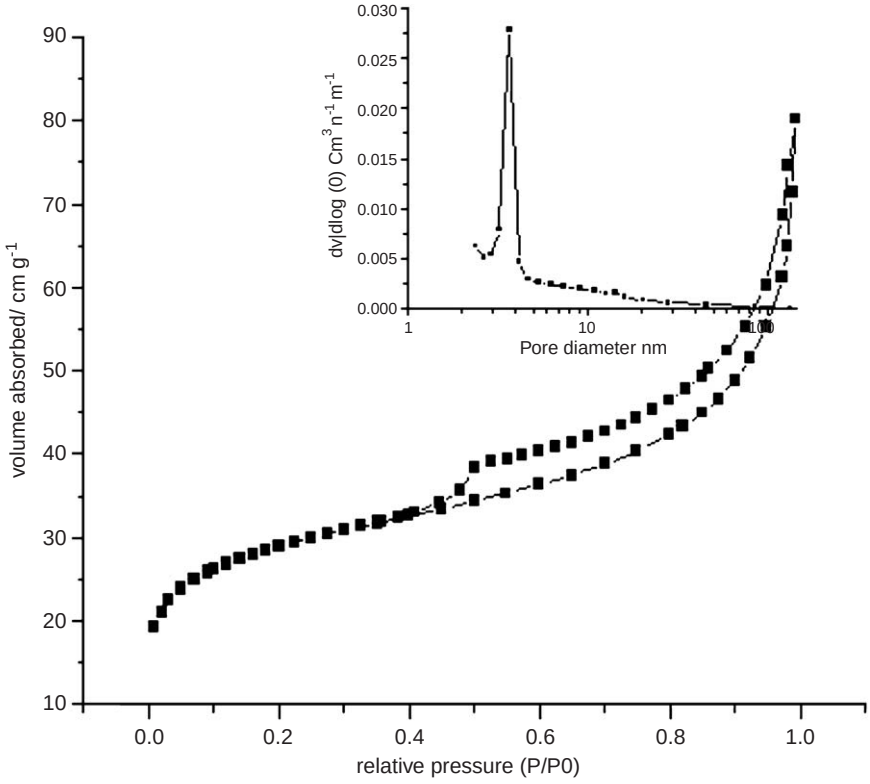

Fig. 6. Nitrogen adsorption/desorption isotherm and Brunauer–Emmett–Teller (BET) pore-size distribution plot (inset) of ZnS hollow spheres.

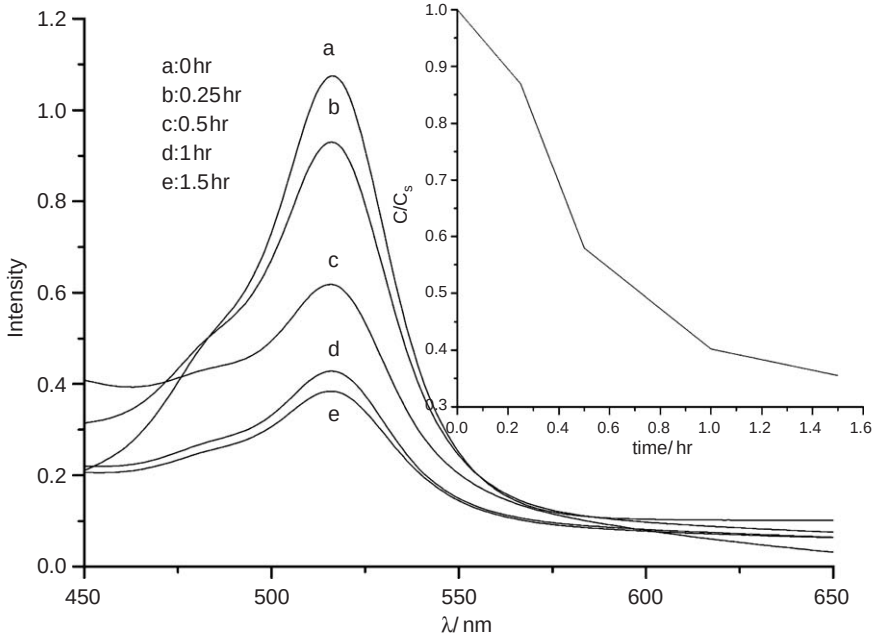

Fig. 7. Absorption spectrum of eosin B aqueous solution with ZnS under the exposure of UV light. Inset is the photocatalytic efficiency curve (C/C_0 vs. time).

at 517 nm can be chosen as the monitored parameter. Fig. 7 shows the absorption spectrum of an aqueous solution of eosin B in the presence of the obtained ZnS under the exposure of UV light for various times. The main absorption peak corresponding to the eosin B molecule at 517 nm decreases gradually as the exposure time increases. From the efficiency curve of the photocatalytic reaction (inset), it can be seen that the photocatalytic efficiency can reach to 65% when the exposure time is up to 1.5 h.

4. Conclusion

ZnO nanospheres were successfully synthesized by hydrothermal method with the presence of poly (sodium-*p*-styrene sulfonate) (PSS) as surfactant at low temperature. The as-synthesized ZnO nanospheres can be evolved to hollow ZnS nanospheres with a nanoporous shell. The hollow ZnS nanospheres has a diameter about 120 nm and the shell thickness about 20–30 nm. The shell was composed of many fine crystallites to form a nanoporous structure. ZnS hollow spheres possess a specific surface area about $97\,m^2\,g^{-1}$ and the average diameter of the pore is about 3.7 nm. Photocatalytic performance shows that the obtained ZnS hollow nanospheres can effectively photo-degrade eosin B, and these hollow ZnS nanospheres can apply as semiconductor photo-catalyst and environment remediation agent to practice applications.

Acknowledgments

This work was financially supported by the National Natural Foundation of China (50103006), the Shanghai ShuGuang Project (01-SG-15) and the Shanghai Nanomaterials Project (0212 nm106).

Appendix A. Supplementary data

Supplementary data associated with this article can be found in the online version at doi:10.1016/j.jssc.2005.09.007.

Reference

[1] Y.C. Zhu, Y. Bando, D.F. Xue, D. Golberg, J. Am. Chem. Soc. 125 (2003) 16196.
[2] Y.W. Zhao, Y. Zhang, H. Zhu, G.C. Hadjipanayis, J.Q. Xiao, J. Am. Chem. Soc. 126 (2004) 6874.
[3] X.J. Chen, H.F. Xu, N.S. Xu, F.F. Zhao, W.J. Lin, G. Lin, Y.L. Fu, Z. L Huang, H.Z. Wang, M.M. Wu, Inorg. Chem. 42 (2003) 3100.
[4] D.F. Moore, Y.D. Zhong, L. Wang, J. Am. Chem. Soc. 126 (2004) 14372.
[5] X.M. Meng, J. Liu, Y. Jiang, W.W. Chen, C.S. Lee, I. Bello, S.T. Lee, Chem. Phys. Lett. 382 (2003) 434.
[6] X.S. Fang, C.H. Ye, X.S. Peng, Y.H. Wang, Y.C. Wu, L.D. Zhang, J. Cryst. Growth 263 (2004) 263.
[7] (a) Q. Li, C. Wang, Appl. Phys. Lett. 83 (2003) 359;
(b) Y.C. Zhu, Y. Bando, D.F. Xue, Appl. Phys. Lett. 82 (2003) 1769;
(c) Y. Jiang, X.M. Meng, J. Liu, Z.Y. Xie, C.S. Lee, S.T. Lee, Adv. Mater. 15 (2003) 323.
[8] X.D. Wang, P.X. Gao, J. Li, C.J. Summers, Z.L. Wang, Adv. Mater. 14 (2002) 1732.
[9] D. Moore, C. Ronning, C. Ma, Z.L. Wang, Chem. Phys. Lett. 385 (2004) 8.
[10] H.Z. Zhang, B. Gilbert, F. Huang, J.F. Banfield, Nature 424 (2003) 1025.
[11] J.S. Hu, L.L. Ren, Y.G. Guo, H.P. Liang, A.M. Cao, L.J. Wan, C.L. Bai, Angew. Chem. Int. Ed. 44 (2005) 1269.
[12] X.Y. Liu, B.Z. Tian, C.Z. Yu, B. Tu, D.Y. Zhao, Chem. Lett. 33 (2004) 522.
[13] S. Yu, M. Yoshimura, Adv. Mater. 14 (2002) 296.
[14] Y. Zhang, Q. Peng, X. Wang, Y.D. Li, Chem. Lett. 33 (2004) 1320.
[15] Y.R. Ma, L.M. Qi, J.M. Ma, H.M. Cheng, Langmuir 19 (2003) 4040.
[16] J.L. Yin, X.F. Qian, J. Yin, M.W. Shi, G.T. Zhou, Mater. Lett. 57 (2003) 3859.
[17] M.L. Breen, A.D. Dinsmore, R.H. Pink, S.B. Qadri, B.R. Ratna, Langmuir 17 (2001) 903.
[18] N.A. Dhas, A. Zaban, A. Gedanken, Chem. Mater. 11 (1999) 806.
[19] Y.J. He, Mater. Res. Bull. 40 (2005) 629.
[20] H. Zhang, S.Y. Zhang, S.A. Pan, G.P. Li, J.G. Hou, Nanotechnology 15 (2004) 945.
[21] Y. Ding, M. Chen, J. Erlebacher, J. Am. Chem. Soc. 126 (2004) 6876.
[22] Y.L. Wang, X.C. Jiang, Y.N. Xia, J. Am. Chem. Soc. 125 (2003) 16176.
[23] C.Y. Lai, B.G. Trewyn, D.M. Jeftinija, K. Jeftinija, S. Xu, S. Jeftinija, V.S.Y. Lin, J. Am. Chem. Soc. 125 (2003) 4451.
[24] F. Li, J. He, W.L. Zhou, J.B. Wiley, J. Am. Chem. Soc. 125 (2003) 16166.
[25] K. Suzuki, K. Ikari, H. Imai, J. Am. Chem. Soc. 126 (2004) 462.
[26] A.D. Smigelskas, E.O. Kirkendall, Trans. AIME 171 (1947) 130.
[27] I. Barin, O. Knacke, Thermochemical Properties of Inorganic Substances, Springer, Berlin, 1973.
[28] Y.D. Yin, R.M. Rioux, C.K. Erdonmez, S. Hughes, G.A. Somorjai, A. Paul Alivisatos, Science 304 (2004) 711.
[29] B. Liu, H.C. Zeng, J. Am. Chem. Soc. 126 (2004) 16744.